A novel building change index for automatic building change detection from high-resolution remote sensing imagery

Xin Huang, Tingting Zhu, Liangpei Zhang & Yuqi Tang

Published online: 29 Sep 2014.

Submit your article to this journal ⬚

Article views: 148

View related articles ⬚

View Crossmark data ⬚

Taylor & Francis
Taylor & Francis Group

A novel building change index for automatic building change detection from high-resolution remote sensing imagery

Xin Huang[a]*, Tingting Zhu[a], Liangpei Zhang[a], and Yuqi Tang[b]

[a]*State Key Laboratory of Information Engineering in Surveying, Mapping and Remote Sensing (LIESMARS), Wuhan University, Wuhan, China;* [b]*School of Geosciences and Info-Physics, Central South University, Changsha, China*

In pace with rapid urbanization, urban areas in many countries are undergoing huge changes. The large spectral variance and spatial heterogeneity within the 'buildings' land cover class, as well as the similar spectral properties between buildings and other urban structures, make building change detection a challenging problem. In this work, we propose a set of novel building change indices (BCIs) by combining morphological building index (MBI) and slow feature analysis (SFA) for building change detection from high-resolution imagery. MBI is a recently developed automatic building detector for high-resolution imagery, which is able to highlight building components but simultaneously suppress other urban structures. SFA is an unsupervised learning algorithm that can discriminate the changed components from the unchanged ones for multi-temporal images. By effectively integrating the information from MBI and SFA, the building change components can be automatically generated. Experiments conducted on the QuickBird 2002–2005 data-set are used to validate the effectiveness of the proposed building change detection framework.

1. Introduction

In recent years, with the increasing availability of very high-resolution images covering the same geographical area, it becomes possible to identify detailed changes that occur at the level of urban structures such as buildings (Gueguen, Soille, and Pesaresi 2011). Due to the socio-economic and environmental issues resulting from the high-speed urbanization, building detection has received increasing attention in recent years in China. As a result, the precise location and identification of changed building structures is one of the most important tasks for updating of an urban land information system. However, few studies in the existing literature have addressed the problem of automatic building change detection from high-resolution remotely sensed imagery.

The complex spatial arrangement and spectral heterogeneity within the class of buildings pose huge challenges to the traditional pixel-based and spectral-based change detection techniques, since the radiometric information alone is insufficient for discrimination between spectrally similar urban structures such as buildings, roads and bare soil. It is therefore necessary to develop context-based methods that can exploit rich spatial information of high-resolution images for accurate change detection (Falco et al. 2013).

Automatic building detection from monocular optical images is a challenging pattern recognition problem, which is also the key for building change analysis. Notable examples of the current building detectors for high-resolution images include the scale-invariant

---

*Corresponding author. Email: huang_whu@163.com

feature transform (SIFT) key-point-based method (Sirmacek and Unsalan 2009) and shadow evidence-based building reconstruction (Liow and Pavlidis 1990). In this study, based on our previous work, a morphological building index (MBI) (Huang and Zhang 2011, 2012) is adopted for automatic building change detection. MBI is of interest because it is an automatic building detector for high-resolution images, which can be rapidly carried out without collection of training samples.

It should be noted that changes in the structure of buildings are related not only to variations in MBI features but also to variations in the spectral domain of multi-temporal images. Change vector analysis (CVA) (Johnson and Kasischke 1998) is a commonly used approach for measuring the spectral difference for change detection. Nevertheless, CVA is a spectral-based change detection technique which tends to yield a number of false alarms when applied to high-resolution images. To this aim, we propose to use slow feature analysis (SFA) (Wiskott and Sejnowski 2002) to measure the multitemporal spectral change. SFA is an unsupervised and nonlinear learning algorithm that extracts invariant and slowly varying features from time series signals. The basic principle of SFA for change detection is to identify the unchanged and changed structures as slowly and fast-varying components, respectively. SFA aims to find the globally optimal solution for a transformed feature space, where the unchanged pixels are suppressed and the changed ones are highlighted (Wu, Du, and Zhang 2014). It has been successfully applied to invariant object recognition (Franzius, Wilbert, and Wiskott 2011) and blind source separation (Blaschke, Zito, and Wiskott 2007). In our previous work, the effectiveness of SFA for change detection was verified based on medium-resolution satellite images (Landsat) (Wu, Du, and Zhang 2014.). However, SFA has not been considered for multitemporal high-resolution image change detection.

The contribution of this study is to propose a set of novel building change indices (BCI) for automatic building change detection by simultaneously taking advantage of MBI and SFA, corresponding to the structural and spectral change components of buildings, respectively. The combined use of MBI-SFA can complement each other and effectively reduce the errors.

2. Methodology

2.1. *MBI*

The complex structures in an urban scene need to be well represented by contextual information, for example size, shape and the relationship between neighbouring spatial units. The notable spectral and structural characteristics of buildings are summarized as follows:

(1) Buildings tend to show high reflectance in the visible spectral bands due to their height and materials.
(2) Buildings as well as their spatially adjacent shadow always present high local contrast.
(3) Buildings are relatively rectangular and isotropic compared to roads.

In this context, MBI is defined by describing the spectral-spatial characteristics of buildings using a series of morphological operators. Computation of MBI can be briefly expressed as the following steps:

Step1: Brightness image. The maximum value of the visible bands for each pixel i is recorded as the brightness $b(i)$:

$$b(i) = \max_{1 \leq k \leq K} (\text{band}_k(i)) \tag{1}$$

where $\text{band}_k(i)$ indicates the digital number (DN) value for pixel i for the kth visible band. K is the total number of the visible spectral bands.

Step2: Differential top-hat profiles (DTPs). DTPs are constructed using a series of multiscale and multidirectional linear structural elements (SEs) to represent the high local contrast of buildings:

$$\text{DTP}(d, s) = |\text{TH}_I(d, s + \Delta s) - \text{TH}_I(d, s)| \tag{2}$$

where s and d indicate the length and direction of the linear SE, respectively, and Δs is the increment of the length. $\text{TH}_I(d, s + \Delta s)$ and $\text{TH}_I(d, s)$ represent the top-hat-by-reconstruction of the brightness image I with a linear SE of length $(s + \Delta s)$ and s, respectively. It should be noted that a linear SE is able to measure the directionality of a structure and, hence, has potential for discrimination between buildings (isotropy) and roads (anisotropy).

Step3: Calculation of MBI.

$$\text{MBI} = \frac{\sum_{d,s} \text{DTP}(d, s)}{D \times S} \tag{3}$$

where D and S are, respectively, the number of directions and number of lengths considered for the DTPs. According to our previous experiments, four directions ($D = 4$) are adequate for describing the geometrical attributes of buildings. The scale parameter s is determined according to the sizes of the buildings and the spatial resolution of the specific image considered. MBI is constructed based on the fact that building structures have large values at most of the scales and in most of the directions in the DTPs, due to their high local contrast and isotropy. In this way, building components are highlighted and backgrounds are suppressed. Readers can refer to Huang and Zhang (2011, 2012) for details of MBI.

2.2. Slow Feature Analysis

Different from our previous work (Wu, Du, and Zhang 2014), in this study, the effectiveness of SFA for high-resolution image is investigated. The rationale of SFA is to extract the slowly varying components from the multitemporal images and find a series of functions to transform the data into a new feature space, where the changed and unchanged information can be effectively separated (Franzius, Wilbert, and Wiskott 2011). Specifically, the spectral change components can be automatically extracted using the following steps.

Step1: Normalization. The bi-temporal multispectral vectors, x and y, are firstly normalized to zero mean and unit variance: $\hat{x}$ and $\hat{y}$, respectively.

Step2: Minimization. The basic principle of SFA is to minimize the difference of multitemporal bands by image transformation:

$$\min\left(\frac{1}{N}\sum_{x,y}\left(g(\hat{\boldsymbol{x}})-\boldsymbol{g}(\hat{\boldsymbol{y}}))^2\right)\right) \tag{4}$$

where N represents the total number of pixels in an image. The function $g(\boldsymbol{x}) = \mathbf{w}^{\mathrm{T}}\boldsymbol{x}$ is used to define the transformation corresponding to the matrix $\mathbf{w}$ from the original spectral space into a new one, where changed and unchanged components can be better separated ('T' represents the matrix transpose).

Step3: Change component extraction. The optimization problem in Equation (4) can be solved by the generalized eigenvalues method (Wu, Du, and Zhang 2014.). Based on the transformation matrix obtained, the SFA variable is subsequently computed for indicating the spectral change component:

$$\mathrm{SFA} = \mathbf{w}^{\mathrm{T}}\boldsymbol{x} - \mathbf{w}^{\mathrm{T}}\boldsymbol{y} \tag{5}$$

Readers can refer to Franzius, Wilbert, and Wiskott (2011) for details of SFA transformation.

2.3. *Building Change Index*

Change detection over urban areas is subject to large amount of false alarms caused by the complex spectral and spatial distribution of urban structures in the multitemporal image scenes. SFA is effective in highlighting the changed areas and at the same time significantly suppressing the false alarms and noise. Consequently, as shown in Figure 1, combination of SFA and MBI has the potential for accurately delineating the changed buildings from urban areas. In this background, we propose a set of novel BCIs by joint use of the SFA (change) and the MBI (buildings). Specifically, three BCIs are constructed based on different strategies:
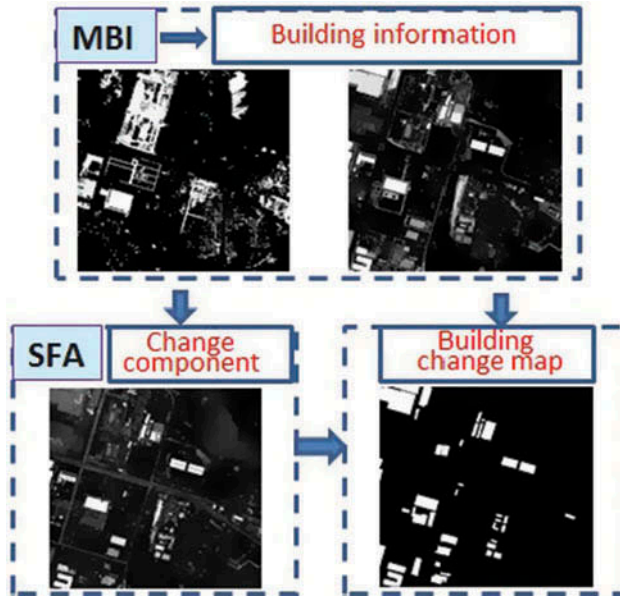

Figure 1.   Integration of MBI and SFA for building change detection.

$$\text{BCI1} = (\text{MBI}(t_1) + \text{MBI}(t_2)) \times (\text{SFA}) \tag{6}$$

where $\text{MBI}(t_1)$ and $\text{MBI}(t_2)$ represent the building components extracted by MBI for time t_1 and t_2, respectively. BCI1 is expressed as sum of $\text{MBI}(t_1) \times (\text{SFA})$ and $\text{MBI}(t_2) \times (\text{SFA})$, which emphasize the disappeared and newly constructed buildings, respectively, since MBI indicates the buildings and SFA corresponds to the change information.

BCI2 is defined as the weighted sum of ΔMBI and SFA:

$$\text{BCI2} = \alpha \times \Delta\text{MBI} + (1 - \alpha) \times (\text{SFA}) \tag{7}$$

where ΔMBI is the change in the MBI, and α is the weighting parameter used to balance the contribution between MBI and SFA features. In this way, the building change information is enhanced by synthesizing both MBI and slowly varying components. For instance, the false and miss alarms derived from ΔMBI can be reduced by simultaneously taking SFA information into account.

BCI3 adopts the *F*-score (F_β) (Sasaki 2007) for integrating ΔMBI and SFA information for building change detection:

$$\text{BCI3} = F_\beta(\Delta\text{MBI}, \text{SFA}) \tag{8}$$

$$\text{with } F_\beta(a, b) = (1 + \beta^2) \frac{a \times b}{\beta^2 \times a + b} \tag{9}$$

F-score is an effective measure for equivalently consider the effects of ΔMBI and SFA. In this study, the value of β is set to 1.

The BCI algorithm can be represented as follows.

(1) Compute the SFA feature image for the stacked multitemporal images using Equation (5), which represents the spectral change component.
(2) Compute the MBI feature image for time 1 and 2 separately using Equation (3): that is, calculate $\text{MBI}(t_1)$ and $\text{MBI}(t_2)$, which represent the multitemporal building information.
(3) Compute the set of BCIs: {BCI1, BCI2, BCI3}.
(4) Apply a threshold to the BCI image, resulting in the initial building change map.
(5) A post-processing is conducted for removing noise.

3. Experiments

3.1. *Data-sets*

The effectiveness of the proposed BCI is assessed on bi-temporal images acquired by the QuickBird satellite in 2002 and 2005 covering the urban area of Wuhan, central China. The test images contain four spectral bands (red, green, blue and near infrared) with a spatial resolution of 2.4 m, and the size for both images is 400 pixels × 1000 pixels. It is a typical urban landscape of China, where both residential and commercial areas consist of high-density buildings and the green space and open areas are insufficient. In recent years, this area is subject to a large amount of change for urban structures (especially for buildings), due to the rapid urban infrastructure construction.

Figure 2(*a*) and (*b*) shows the 2002 and 2005 QuickBird image pairs of Wuhan urban areas, respectively. An accurate geometric registration for the test images is conducted based
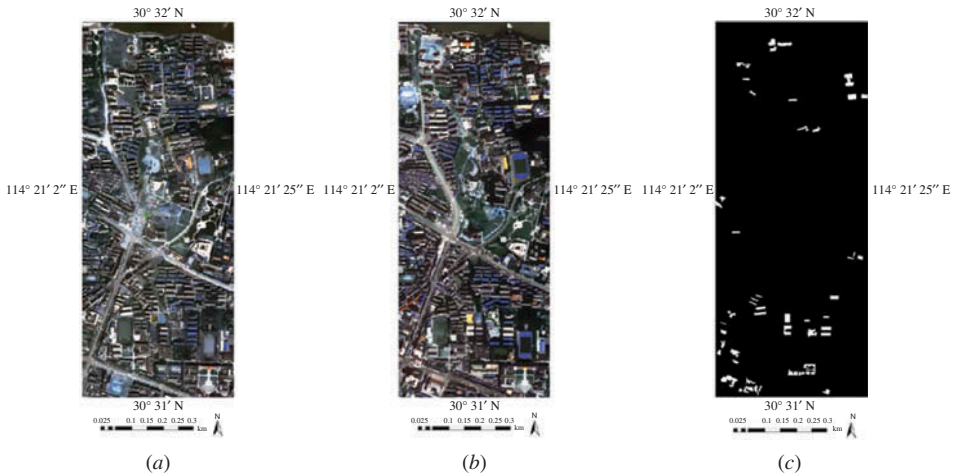
Figure 2.   QuickBird images for the urban area of Wuhan in (a) 2002 and (b) 2005, and (c) the reference of the changed buildings, which was manually delineated based on a careful ground surveying and investigation for the accuracy assessment (the changed buildings and other back-grounds are in white and black, respectively).

on 12 ground control points, leading to a residual average misregistration error less than one pixel. The ground truth reference (Figure 2(c)) of the changed buildings is manually deli-neated based on a careful ground surveying and investigation for the accuracy assessment, where the changed buildings and other backgrounds are in white and black, respectively.

3.2.   Results

The ΔMBI and SFA features as well as the bi-temporal MBI images are displayed in Figure 3. The scale parameter s for the MBI is set from 1 to 30 with an interval of 2 ($\Delta s = 2$), according to the sizes of buildings and the spatial resolution of the test images. It can be clearly seen that ΔMBI image can indicate the presence of changed building components correctly. SFA is able to highlight the spectral change information in this area, most of which corresponds to buildings. By comparing the Figure 3(c) and (d), it can be found that some changed building structures are missed by ΔMBI due to the errors from the calculation of MBI. This is understandable considering that MBI is an automatic building index and its accuracy is related to the radiometric conditions of an image (Huang and Zhang 2011, 2012). In such a case, the signals for changed buildings can be complemented by the SFA image. On the other hand, the SFA feature is subject to a number of false alarms involving non-building urban structures such as soil and roads. Consequently, the ΔMBI and SFA features can complement each other and improve the performance of building change detection.

The accuracy assessment is based on the following four scores:

(1) Correctness: Percentage of correctly detected changed building pixels;
(2) Omission error: Percentage of changed building pixels which are identified as unchanged;
(3) Commission error: Percentage of unchanged pixels that are identified as changed;
(4) Overall error: the average of omission and commission errors.
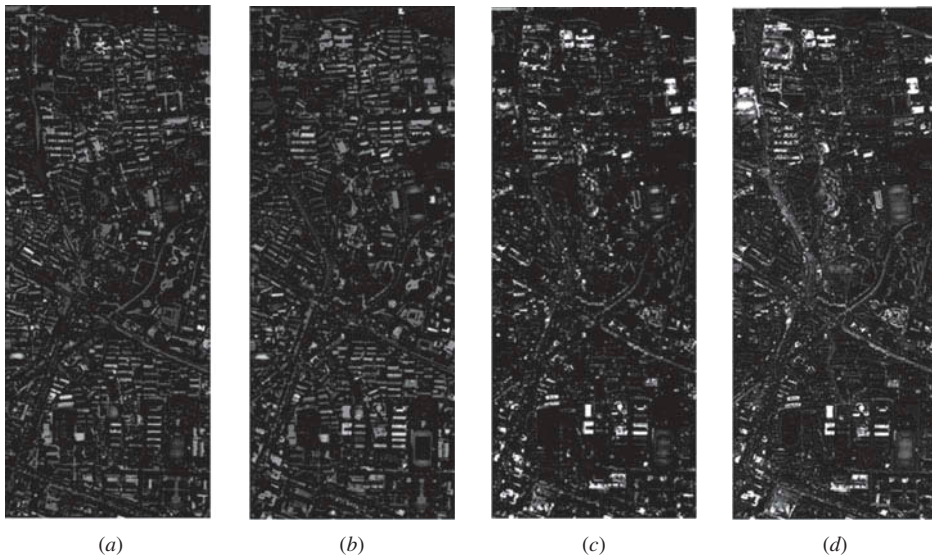
Figure 3. (a) and (b) are the MBI feature images at the year of 2002 and 2005, respectively; (c) and (d) are the ΔMBI and SFA feature images, respectively. (The area covered by these images is the same as that covered by Figure 2).

Table 1. Accuracy assessment and comparison for the methods listed (PP = post-processing).

Methods	Correctness	Omission error	Commission error	Overall error
BCI1	0.8964	0.1036	0.1236	0.1136
BCI1 with PP	0.8961	0.1038	0.1054	0.1046
BCI2	0.8873	0.1126	0.1641	0.1384
BCI2 with PP	0.8878	0.1122	0.1548	0.1335
BCI3	0.8768	0.1231	0.1264	0.1248
BCI3 with PP	0.8774	0.1226	0.1162	0.1194
SFA	0.8611	0.1388	0.1616	0.1502
SFA with PP	0.8592	0.1408	0.1588	0.1498
MBI	0.8671	0.1328	0.1059	0.1194
MBI with PP	0.8696	0.1303	0.0904	0.1103

The results are presented in Table 1, where PP denotes the post-processing with the area-based thresholding used to remove pepper-and-salt noise. Note that the SFA and MBI methods indicate the building change detection based on SFA and MBI feature, respectively, while the BCIs are based on their combination. The threshold values corresponding to the smallest overall errors are selected for the building change detection.

From the table, it can be found that:

(1) The three BCIs are effective in indicating the changed building information in terms of accuracy scores. Among those, BCI1 achieves the highest correctness and the lowest overall error.
(2) The post-processing is appropriate as it is able to maintain the level of correctness and at the same time reduce the commission error.

(3) BCIs outperform SFA and MBI, showing that the combination of these two information sources can complement each other and further improve the accuracy of building change detection. Note that SFA alone is not a suitable approach for building change detection since it provides 16.2% commission error, which is understandable since SFA is not only related to the change of buildings, but also to other urban structures such as soil and roads.

Figure 4 shows how the threshold values affect the change detection accuracy. It can be seen that the three BCIs are effective for integrating the information from MBI and SFA, since they achieve higher correctness and lower error than their individual use. It can also be noticed that among the three BCIs, BCI1 provides the best performance in terms of the accuracy curves.
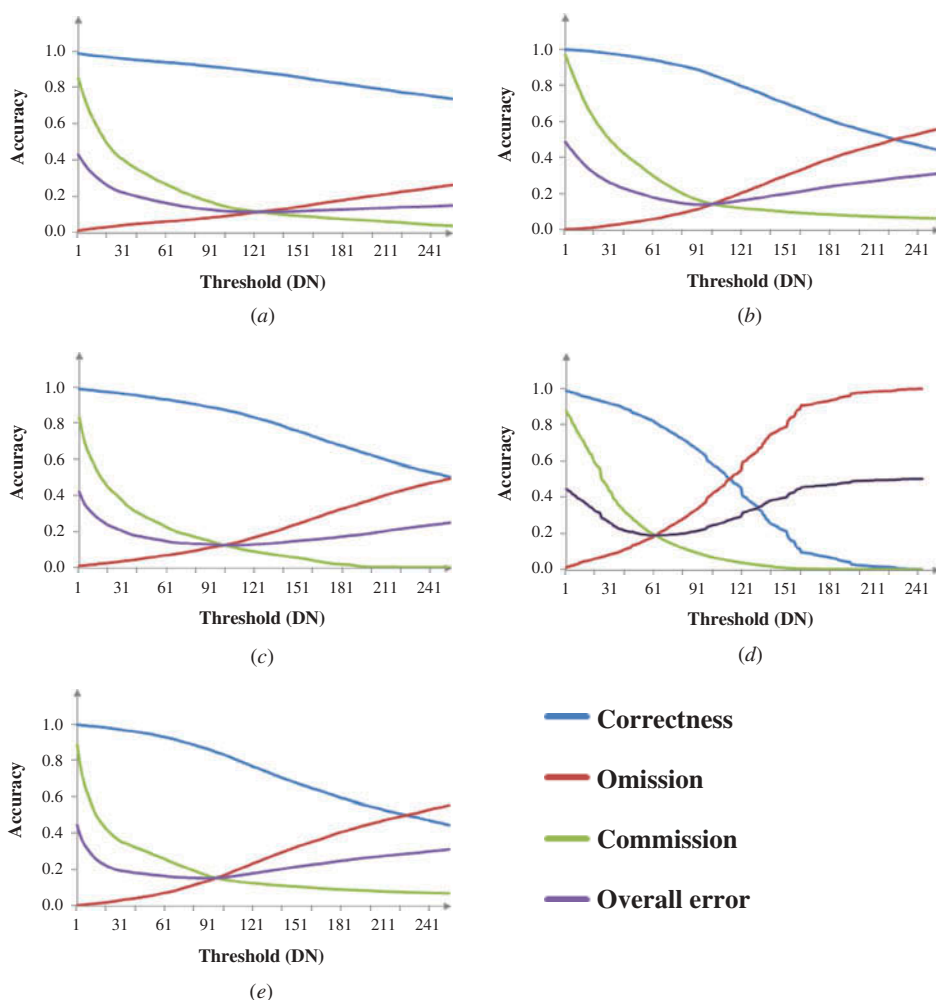

Figure 4. Relationship between threshold values and change detection accuracies. (a), (b) and (c) are the results for BCI1, BCI2 and BCI3, respectively, while (d) and (e) are the results of ΔMBI and SFA, respectively. The threshold is a predefined value used to determine whether the building change takes place.
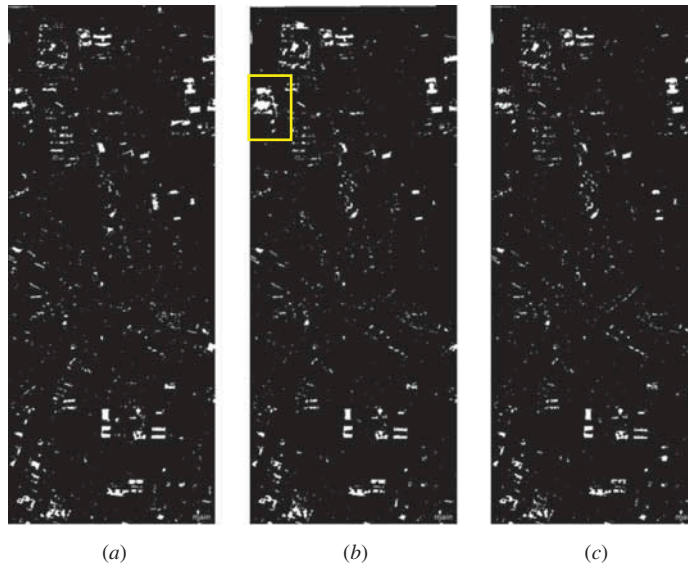
Figure 5. (a), (b) and (c) represent the change detection results for BCI1, BCI2 and BCI3, respectively. As indicated in the yellow rectangular box, the bright soil in this region is highlighted as changed buildings by BCI2, resulting in a larger commission error. (The area covered by these images is the same as that covered by Figure 2. The changed buildings and other backgrounds are in white and black, respectively.).

In order to further analyse the experimental results, the change detection maps are displayed in Figure 5 for a visual inspection. In particular, as indicated in the yellow rectangular box, the bright soil in this region is highlighted as changed buildings by BCI2, resulting in a larger commission error. On the other hand, however, this false alarm is overcome by BCI1 and BCI3. The multiplication (BCI1) and the *F*-measure (BCI3) are more appropriate for combining SFA and MBI than the weighted sum.

4. Discussions and conclusions

In this study, a series of novel BCIs, combining the SFA and MBI features, are proposed for automatically indicating the building change information from high-resolution imagery. SFA is able to extract the spectral change components, and MBI is used to focus the change detection on building structures. Specifically, three strategies are proposed for combining the SFA and MBI information, based on multiplication (BCI1), weighted sum (BCI2) and *F*-measure (BCI3).

The experiments show that the proposed BCIs are effective in integrating the SFA and MBI features since they achieve higher correctness and lower errors than individual use of SFA and ΔMBI. In particular, the BCI1 provides the best result in this experiment, that is, the highest correctness (90%) and the lowest overall error (10%). The computation time is 44.09, 44.13 and 44.09 seconds for the three BCIs, respectively, which is approximately equal to the sum of the time for calculating MBI (12.76 s) and SFA (31.32 s).

It should be noted that the proposed BCIs are unsupervised building change detectors. This is meaningful considering the current building change detection highly relies on

manual operation, which is time-consuming for the database update of the urban building information.

In future, we plan to apply the proposed BCIs to the real process of updating the building database of an area. Another potential application is to extend the pixel-based building change detection to the object-based or block-based approach, in order to impose the semantic information or rules on the results and further enhance the change detection accuracy.

Funding

References

Blaschke, T., T. Zito, and L. Wiskott. 2007. "Independent Slow Feature Analysis and Nonlinear Blind Source Separation." *Neural Computation* 19: 994–1021. doi:10.1162/neco.2007.19.4.994.

Falco, N., M. Mura, F. Bovolo, J. A. Benediktsson, and L. Bruzzone. 2013. "Change Detection in VHR Images Based on Morphological Attribute Profiles." *IEEE Geoscience and Remote Sensing Letters* 10: 636–640. doi:10.1109/LGRS.2012.2222340.

Franzius, M., N. Wilbert, and L. Wiskott. 2011. "Invariant Object Recognition and Pose Estimation with Slow Feature Analysis." *Neural Computation* 23: 2289–2323.

Gueguen, L., P. Soille, and M. Pesaresi. 2011. "Change Detection Based on Information Measure." *IEEE Transactions on Geoscience and Remote Sensing* 49: 4503–4515. doi:10.1109/TGRS.2011.2141999.

Huang, X., and L. Zhang. 2011. "A Multidirectional and Multiscale Morphological Index for Automatic Building Extraction from Multispectral Geoeye-1 Imagery." *Photogrammetric Engineering and Remote Sensing* 77: 721–732. doi:10.14358/PERS.77.7.721.

Huang, X., and L. Zhang. 2012. "Morphological Building/Shadow Index for Building Extraction from High-Resolution Imagery over Urban Areas." *IEEE Journal of Selected Topics in Applied Earth Observations and Remote Sensing* 5: 161–172. doi:10.1109/JSTARS.2011.2168195.

Johnson, R. D., and E. S. Kasischke. 1998. "Change Vector Analysis: A Technique for the Multispectral Monitoring of Land Cover and Condition." *International Journal of Remote Sensing* 19: 411–426. doi:10.1080/014311698216062.

Liow, Y.-T., and T. Pavlidis. 1990. "Use of Shadows for Extracting Buildings in Aerial Images." *Computer Vision, Graphics, and Image Processing* 49: 242–277. doi:10.1016/0734-189X(90)90139-M.

Sasaki, Y. 2007. "The Truth of the F-Measure." Accessed April 21, 2014. http://www.cs.odu.edu/~mukka/cs795sum09dm/Lecturenotes/Day3/F-measure-YS-26Oct07.pdf.

Sirmacek, B., and C. Unsalan. 2009. "Urban-Area and Building Detection Using SIFT Keypoints and Graph Theory." *IEEE Transactions on Geoscience and Remote Sensing* 47: 1156–1167. doi:10.1109/TGRS.2008.2008440.

Wiskott, L., and T. J. Sejnowski. 2002. "Slow Feature Analysis: Unsupervised Learning of Invariances." *Neural Computation* 14: 715–770. doi:10.1162/089976602317318938.

Wu, C., B. Du, and L. Zhang. 2014. "Slow Feature Analysis for Change Detection in Multispectral Imagery." *IEEE Transactions on Geoscience and Remote Sensing* 52: 2858–2874. doi:10.1109/TGRS.2013.2266673.